Low Overhead Universal Quantum Computation with Triorthogonal Codes

Dawei Jiao[1], Mahdi Bayanifar[1], Alexei Ashikhmin[2], and Olav Tirkkonen[1]

[1]Department of Communications and Networking, Aalto University, Finland
[2]Nokia Bell Labs, Murray Hill, New Jersey, USA

We study the use of triorthogonal codes for universal fault-tolerant quantum computation and propose two methods to circumvent the Eastin-Knill theorem, which prohibits any single quantum error-correcting code from supporting both universality and a transversal gate set. We show that our methods reduce the resource overhead compared with existing fault-tolerant protocols. We develop a simple fault-tolerant implementation of the logical Hadamard gate for triorthogonal codes by exploiting the fact that they have transversal controlled-Z (CZ) gates, resulting in a circuit with reduced overhead. We also introduce a procedure for generating a symmetric Calderbank-Shor-Steane code paired with a triorthogonal code, which allows CNOT and CZ gate transversality across the pair of codes. In addition, we present logical state teleportation circuits that transfer encoded states between the two codes, allowing all logical operations to be performed transversally. Our methods can be integrated into the Steane error correction framework without incurring additional resource cost. Finally, using the 15-qubit code as an example, we demonstrate that our protocols significantly reduce the gate overhead compared with other existing methods. These results highlight the potential of combining distinct code structures to achieve low-overhead, universal fault-tolerant quantum computation.

1 Introduction

Quantum error correcting codes (QECCs) are crucial for suppressing physical errors in large quantum systems, through encoding information into a protected subspace of a larger Hilbert space [1, 2, 3]. To ensure reliable computation, quantum logical operations must be implemented fault-tolerantly, so that a single physical error does not spread uncontrollably and become unrecoverable [4, 5]. However, fault-tolerance alone is not sufficient, universal quantum computation also requires a gate set capable of implementing arbitrary unitary operations. Transversal gates are highly desirable due to their inherent error-localization properties, but as shown by the Eastin-Knill theorem [6], no QECC supports a universal gate set composed entirely of transversal operations.

To circumvent this limitation, several strategies have been proposed. The standard approach uses magic states [7, 8], where non-Clifford gates, such as the **T**-gate, are implemented by gate teleportation using specially prepared ancillary states. When combined with codes supporting transversal Clifford gates this enables universal fault-tolerant computation. However, preparing high-fidelity magic states through distillation is resource

Dawei Jiao: dawei.jiao@aalto.fi

costly, often requiring orders of magnitude more qubits and gates than other logical operations [9].

An alternative strategy focuses on codes that admit transversal non-Clifford gates, such as triorthogonal codes with transversal **T** and controlled-controlled-Z (CCZ) gates [7, 10], while using additional techniques to implement non-transversal Clifford gates fault-tolerantly [11, 12, 13, 14]. This direction is promising, and has a lower qubit resource cost, as Clifford gates are generally easier to realize and correct in hardware.

In this paper, we follow the latter approach. We propose two methods to achieve fault-tolerant universal computation using triorthogonal codes. The first one is based on a novel fault-tolerant logical Hadamard gate protocol for triorthogonal codes. The proposed protocol requires less resources and does not change the code space compared to [11, 13]. In particular, our protocol does not use CCZ gates, and therefore it requires smaller overhead compared to [13]. The protocol also reduces the number of single-qubit physical operations compared with [11]. Our second method is base on a novel protocol for teleporting logical states between a triorthogonal code and a symmetric Calderbank-Shor-Steane (CSS) code derived from it, using only transversal operations. This enables all Clifford and non-Clifford gates to be performed in codes where they are natively transversal. While working on this manuscript we discovered that in some sense similar approach was proposed recently in [15]. However, our protocol is not identical to the one from [15], and it is more general and not limited by particular types of codes. Which protocol is more efficient depends on the relative frequencies of the Hadamard and other Clifford gates in a given quantum algorithm. It is also important to note that our protocol can be integrated into the Steane error correction framework [16], incurring no additional overhead in terms of qubits or gates compared to standard syndrome extraction. Using the $[[15, 1, 3]]$ triorthogonal code [7] as an example, we demonstrate the gate and qubit resource cost with and without state preparation. We compare the results with methods from [11, 15, 17]. The results show that our method reduces the gate overhead significantly.

The rest of the paper is organized as follows: Section 2 introduces preliminaries on CSS codes, transversal gates, triorthogonal codes, and the Steane error correction method. Section 3 reviews relevant prior work and presents our optimized Hadamard gate circuit. In Section 4, we describe how to construct symmetric CSS codes from triorthogonal codes and examine their transversal gate sets, using an $[[15, 1, 3]]$ code as an example. Section 4.2 introduces our teleportation circuits for transferring logical states between the two codes. Section 5 demonstrates how our approach can be merged within the Steane error correction procedure without additional resources. Finally, in Section 6, we use the 15-qubit code as an example to demonstrate that our protocol reduces gate overhead as compared with other deterministic methods.

2 Preliminaries

2.1 CSS Codes

CSS quantum error correction codes can be constructed based on two classical binary linear codes $\mathcal{C}_1\,[n, k_1, d_1]$ and $\mathcal{C}_2\,[n, k_2, d_2]$, such that $\mathcal{C}_2^{\perp} \subset \mathcal{C}_1$, with $\mathcal{C}_2^{\perp}$ the dual space of $\mathcal{C}_2$. A quantum $[[n, k, d]]$ CSS code $\mathcal{Q} = \mathrm{CSS}\,(\mathcal{C}_1, \mathcal{C}_2)$ is defined as a 2^k-dimensional linear subspace of $\mathbb{C}^{2^n}$ with orthonormal basis [1]

$$|\psi\rangle_L = \frac{1}{\sqrt{|\mathcal{C}_2^{\perp}|}} \sum_{\mathbf{y}\in\mathcal{C}_2^{\perp}} |\mathbf{x}_\psi + \mathbf{y}\rangle, \tag{1}$$

where $\boldsymbol{\psi} \in \mathbb{F}_2^k$ and $\mathbf{x}_{\boldsymbol{\psi}} = \boldsymbol{\psi}\mathbf{A}$, where $\mathbf{A} \in \mathbb{F}_2^{k\times n}$ is a full-rank mapping matrix which is a generator of the quotient group $\mathcal{C}_1/\mathcal{C}_2^{\perp}$, i.e., $\mathbf{A} \cong \mathcal{C}_1/\mathcal{C}_2^{\perp}$. Note that $k = k_1 + k_2 - n$ and the code minimum distance is $d = \min(d_1', d_2')$, where $d_1' = \min\{\omega_H(\mathbf{c})|\mathbf{c} \in \mathcal{C}_1/\mathcal{C}_2^{\perp}\}$ and $d_2' = \min\{\omega_H(\mathbf{c})|\mathbf{c} \in \mathcal{C}_2/\mathcal{C}_1^{\perp}\}$.

Pauli matrices for a single qubit system are defined as

$$\mathbf{X} \triangleq \begin{bmatrix} 0 & 1 \\ 1 & 0 \end{bmatrix}, \ \mathbf{Z} \triangleq \begin{bmatrix} 1 & 0 \\ 0 & -1 \end{bmatrix} \ \mathbf{Y} \triangleq \begin{bmatrix} 0 & -i \\ i & 0 \end{bmatrix}, \tag{2}$$

where $i \triangleq \sqrt{-1}$. Pauli errors acting on n qubits have the form $\mathbf{E}(\mathbf{a}, \mathbf{b}) = i^{\mathbf{a}\mathbf{b}^T}\mathbf{D}(\mathbf{a}, \mathbf{b})$, where $\mathbf{D}(\mathbf{a}, \mathbf{b}) = \mathbf{X}^{a_1}\mathbf{Z}^{b_1} \otimes ... \otimes \mathbf{X}^{a_n}\mathbf{Z}^{b_n}$ and $\mathbf{a} = [a_1, ..., a_n]$, $\mathbf{b} = [b_1, ..., b_n]$ are binary vectors. We denote by γ the homomorphism defined by $\gamma(i^{\kappa}\mathbf{D}(\mathbf{a}, \mathbf{b})) = [\mathbf{a}, \mathbf{b}]$, for $\kappa \in \{0, 1, 2, 3\}$.

A CSS$(\mathcal{C}_1, \mathcal{C}_2)$ code, defined above, is an $[[n, k]]$ stabilizer code [1] whose $n-k$ generators correspond to binary vectors $\mathbf{g}_i$, $i = 1, ..., n-k$ in the form $[\mathbf{a}, \mathbf{0}]$ or $[\mathbf{0}, \mathbf{b}]$, where $\mathbf{0} \in \mathbb{F}_2^n$ is the all zero vector. Combining vectors $\mathbf{a}$ and $\mathbf{b}$, we obtain parity check matrices $\mathbf{H}(\mathcal{C}_2)$ and $\mathbf{H}(\mathcal{C}_1)$ of codes $\mathcal{C}_2$ and $\mathcal{C}_1$ respectively. Putting these matrices together, we obtain the matrix $\mathbf{G}^{\mathcal{Q}}$, the matrix of stabilizer generators of CSS$(\mathcal{C}_1, \mathcal{C}_2)$:

$$\mathbf{G}^{\mathcal{Q}} = \left[\begin{array}{cc} \mathbf{H}(\mathcal{C}_2) & \mathbf{0} \\ \hline \mathbf{0} & \mathbf{H}(\mathcal{C}_1) \end{array}\right]. \tag{3}$$

The binary matrix $\mathbf{G}^{\mathcal{Q}}$ has dimension $(n-k) \times 2n$, which implies that $\mathcal{Q}$ encodes k logical qubits into n physical qubits. A CSS code is called *symmetric* if $\mathcal{C}_1 = \mathcal{C}_2$.

2.2 Transversality

Let $\mathbf{U}$ be a $2^m \times 2^m$ operator acting on m qubits. The following definition of a *U-transversal code* is widely used in the literature. Let $\hat{\mathbf{U}}_i$ be the $2^{mn} \times 2^{mn}$ operator that applies $\mathbf{U}$ to qubits with indices $\{i + ln : 0 \le l \le m-1\}$ among mn qubits. Assume that we have an $[[n, k]]$ stabilizer codes $\mathcal{Q}$ and $\mathbf{U}_{\text{Enc}}$ is an encoding operator of $\mathcal{Q}$. $\mathcal{Q}$ is $\mathbf{U}$-transversal if:

$$\left(\prod_{i=1}^{n}\hat{\mathbf{U}}_i\right)\bigotimes_{j=1}^{m}(\mathbf{U}_{\text{Enc}}|\boldsymbol{\psi}_j\rangle|0\ldots0\rangle) = \left(\bigotimes_{s=1}^{m}\mathbf{U}_{\text{Enc}}\right)\left(\prod_{i=1}^{k}\hat{\mathbf{U}}_i\right)\bigotimes_{j=1}^{m}(|\boldsymbol{\psi}_j\rangle|0\ldots0\rangle), \tag{4}$$

where $|\boldsymbol{\psi}_j\rangle \in \mathbb{C}^{2^k}$ are logical states before encoding, and the $|0\ldots0\rangle$ state corresponds to the $n-k$ physical qubits initialized in the $|0\rangle$ state for the encoding process.

Different stabilizer codes have different sets of transversal gates, e.g., any CSS codes is controlled-NOT (CNOT) gate transversal. Furthermore, any symmetric CSS code has transversality for all Clifford gates. For non-Clifford gate, a very useful non-Clifford gate is the $\mathbf{T}$-gate:

$$\mathbf{T} = \begin{bmatrix} 1 & 0 \\ 0 & e^{i\pi/4} \end{bmatrix}.$$

Certain non-symmetric CSS codes belonging to the family of triorthogonal codes are T-transversal [7].

In [18], we proposed the following generalization of the standard definition (4) of transversality within the same code. Assume that we have m $[[n, k]]$ stabilizer codes $\mathcal{Q}_j$, $j = 1, \ldots, m$, and $\mathbf{U}_{\text{Enc,j}}$ is an encoding operator of $\mathcal{Q}_j$. Codes $\mathcal{Q}_1, \ldots, \mathcal{Q}_m$ are $\mathbf{U}$-transversal if:

$$\left(\prod_{i=1}^{n}\hat{\mathbf{U}}_i\right)\bigotimes_{j=1}^{m}(\mathbf{U}_{\text{Enc,j}}|\boldsymbol{\psi}_j\rangle|0\ldots0\rangle) = \left(\bigotimes_{s=1}^{m}\mathbf{U}_{\text{Enc,s}}\right)\left(\prod_{i=1}^{k}\hat{\mathbf{U}}_i\right)\bigotimes_{j=1}^{m}(|\boldsymbol{\psi}_j\rangle|0\ldots0\rangle). \tag{5}$$

In other words, the standard definition (4) assumes **U** operation between m code states of the same code $\mathcal{Q}$, and (5) assumes **U** operation between m code states of m different codes, $\mathcal{Q}_1, \ldots, \mathcal{Q}_m$. We show in the following sections that this opens up a number of new opportunities and can be very useful for fault-tolerant computations.

In [18] we considered the case of $m = 2$ in details and formulated the necessary and sufficient conditions for code pairs to be CNOT and CZ transversal. The conditions for realizing a transversal logical CNOT from $\mathrm{CSS}(\mathcal{C}_1, \mathcal{C}_2)$ to $\mathrm{CSS}(\mathcal{C}_3, \mathcal{C}_4)$ are:

$$\mathcal{C}_1/\mathcal{C}_2^{\perp} \cong \mathcal{C}_3/\mathcal{C}_4^{\perp}, \quad \mathcal{C}_2^{\perp} \subseteq \mathcal{C}_4^{\perp}. \tag{6}$$

Similarly, we have CZ gate transversality between $\mathrm{CSS}(\mathcal{C}_1, \mathcal{C}_2)$ and $\mathrm{CSS}(\mathcal{C}_3, \mathcal{C}_4)$ iff:

$$\mathbf{x}^A \mathbf{z}^T + \mathbf{y}\left(\mathbf{x}^B + \mathbf{z}\right)^T = 0 \qquad \forall\, \mathbf{x}^A \in \mathcal{C}_1/\mathcal{C}_2^{\perp},\, \mathbf{x}^B \in \mathcal{C}_3/\mathcal{C}_4^{\perp},\, \mathbf{y} \in \mathcal{C}_2^{\perp},\, \mathbf{z} \in \mathcal{C}_4^{\perp} \tag{7}$$

$$\mathbf{A}\mathbf{B}^T = \mathbf{I}, \tag{8}$$

where $\mathbf{A}, \mathbf{B} \in \mathbb{F}_2^{k \times n}$, $\mathbf{A} \cong \mathcal{C}_1/\mathcal{C}_2^{\perp}$, $\mathbf{B} \cong \mathcal{C}_3/\mathcal{C}_4^{\perp}$ are two mapping matrices, of the kind discussed after (1). Often, it is more convenient to use the following sufficient conditions:

$$\mathcal{C}_1/\mathcal{C}_2^{\perp} \subset \mathcal{C}_4, \quad \mathcal{C}_3 \subseteq \mathcal{C}_2, \quad \mathbf{A}\mathbf{B}^T = \mathbf{I}. \tag{9}$$

2.3 Triorthogonal Code

Triorthogonal codes are a special type of CSS codes, which are generated by a triorthogonal matrix. A matrix $\mathbf{G} = [G_{ij}] \in \mathbb{F}_2^{m \times n}$ is called *triorthogonal* if

$$\sum_{i=1}^{n} G_{ai} G_{bi} = 0 \bmod 2, \text{ for any } a \neq b\,, \tag{10}$$

$$\sum_{i=1}^{n} G_{ai} G_{bi} G_{ci} = 0 \bmod 2, \text{ for any distinct } a, b, c \tag{11}$$

see [19]. By row permutation, we get

$$\mathbf{G} = \left[\frac{\mathbf{G}_1}{\mathbf{G}_0}\right], \tag{12}$$

where $\mathbf{G}_1$ and $\mathbf{G}_0$ formed by all odd and even weight rows of $\mathbf{G}$, respectively.

Definition 1. *A triorthogonal matrix* $\mathbf{G}$ *defines an* $[[n, k, d]]$ *triorthogonal* $\mathrm{CSS}\,(\mathcal{C}_1, \mathcal{C}_2)$ *code with stabilizers*

$$\mathbf{G}^{\mathcal{Q}^T} = \left[\begin{array}{cc} \mathbf{G}_0 & \mathbf{0} \\ \hline \mathbf{0} & \mathbf{G}^{\perp} \end{array}\right], \tag{13}$$

where k *is the number of rows of* $\mathbf{G}_1$, $\mathbf{G}$ *and* $\mathbf{G}_0^{\perp}$ *are generator matrices of* $\mathcal{C}_1$ *and* $\mathcal{C}_2$ *respectively. For a matrix* $\mathbf{G}$ *we denote by* $\mathbf{G}^{\perp}$ *a generator matrix of the dual space of* $\mathbf{G}$.

It is shown in [10] that if a triorthogonal CSS code $\mathcal{Q}^T$ is Pauli **X**-transversal then $\mathcal{Q}^T$ is also **T**-transversal. We shall call such codes *T-triorthogonal*.

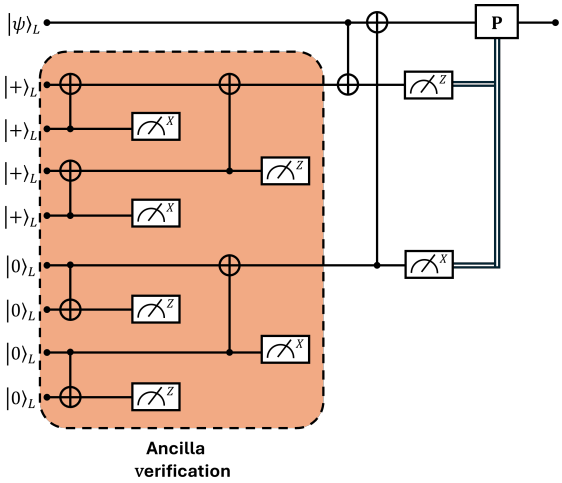

Figure 1: The Steane error correction syndrome extraction circuit. Two ancilla blocks (the second and sixth lines) encoded in logical $|+\rangle_L$ and $|0\rangle_L$ states to load the physical errors from data qubits. Error syndromes can be obtained by measuring ancillas. Additional six ancilla blocks are used to prevent high-weight physical errors on ancilla qubits from propagating to data qubits.

2.4 Steane Error Correction Method

In what follows we shall use T-triorthogonal codes within the Steane error correction method [16], which can be briefly described as follows.

For CSS code $\mathrm{CSS}(\mathcal{C}_1, \mathcal{C}_2)$, the Steane error correction procedure begins with preparing an ancilla block in the $|+\rangle_L$ state. A transversal logical CNOT gate is applied from the data to the ancilla block, resulting in $\mathbf{CNOT}|\psi\rangle_L|+\rangle_L = |\psi\rangle_L|+\rangle_L$. Next, the physical ancilla qubits are measured in the Pauli $\mathbf{Z}$-basis.

If there are no physical Pauli $\mathbf{X}$-errors on data qubits, the logical CNOT gate leaves the state unchanged, and the measurement outcome is a random binary codeword from $\mathcal{C}_1$. Otherwise Pauli $\mathbf{X}$ errors will propagate to the ancilla qubits, resulting in a corrupted codeword. The error syndrome reveals the error locations, and due to the correlation introduced by the CNOT, the recovery operation can be applied to the data block to restore the logical state.

The procedure for Pauli $\mathbf{Z}$ error correction is similar. It uses an ancilla block initialized in the logical $|0\rangle_L$ state and the transversal CNOT gate from ancilla to the data block.

Preparation of the logical $|0\rangle_L$ and $|+\rangle_L$ state may not be fault-tolerant, allowing low-weight errors to spread to data qubits via CNOT gates. To prevent this, ancilla blocks are verified using extra qubits. As shown in Fig. 1, implementing Steane error correction for an $[[n, k, d]]$ CSS code requires eight ancilla blocks per correction round [20]. If non-trivial syndromes are detected, the ancilla blocks are discarded and re-prepared. Ancilla overhead can be reduced by using alternative fault-tolerant strategies, such as flag qubits or stabilizer measurements [21, 22].

3 Logical Hadamard Gate by CZ Gate

In this section, we propose an improved technique for the logical Hadamard gate for tri-orthogonal codes, compared to techniques proposed in [13, 11]. Our technique reduces the overhead while maintaining fault-tolerance. The combination of our fault-tolerant Hadamard gate procedure and $\mathbf{T}$-gate transversality enables universal fault-tolerant quan-

tum computation with T-triorthogonal codes. This fault-tolerant logical Hadamard gate circuit can be merged into Steane error correction procedure without additional cost. More details can be found in Sec. 5.

In [13], the authors demonstrated that codes admitting transversal CCZ gates can implement a logical Hadamard gate $\mathbf{H}$ over a code state $|\psi\rangle_L$. For this, one prepares additional code states $|1\rangle_L$ and $|+\rangle_L$, then acts on them as $\mathbf{CCZ}|1\rangle_L|+\rangle_L|\psi\rangle_L$ transforming $|+\rangle_L$ into $\mathbf{H}|\psi\rangle_L$. This scheme enables a universal gate set $\{\mathbf{CCZ}, \mathbf{H}\}$. However, logical Hadamard fidelity is constrained by the CCZ gate, and the implementation requires three code blocks in total.

An alternative approach was presented in [11]. A triorthogonal code is assisted by a gauge code for achieving a transversal Hadamard gate. This method requires only one ancilla code block and transversal CNOT gates. Furthermore, when integrated with Steane error correction, the ancilla block can be merged into the syndrome extraction procedure. The disadvantage of this approach is that transversal Hadamard gates do not preserve the code space. Therefore, when it is followed by error correction, 6 out of 10 error syndrome bits are needed for mapping the state back to the code space, which reduces the X-error correction capability from correct all weight-3 errors to weight-1 errors.

We now propose a technique for implementing the logical Hadamard gate transversally that requires a single ancilla block and is simpler than the previously discussed methods. Rather than employing a transversal CCZ gate for achieving a logical CZ, we reduce the overhead while preserving the code space by using an inherited CZ-transversality of triorthogonal codes, as detailed in the following theorem.

Theorem 1. *Any triorthogonal code $\mathcal{Q}^T$ is CZ transversal.*

Proof. Consider using the same triorthogonal code within two code blocks, $\mathcal{Q}^T \otimes \mathcal{Q}^T = \mathrm{CSS}(\mathcal{C}_1, \mathcal{C}_2) \otimes \mathrm{CSS}(\mathcal{C}_3, \mathcal{C}_4)$, with $\mathcal{C}_1 = \mathcal{C}_3$ and $\mathcal{C}_2 = \mathcal{C}_4$ with generators $\mathbf{G}$ and $\mathbf{G}_0^{\perp}$, respectively. Note that $\mathcal{C}_1^{\perp} \perp \mathcal{C}_2$, since $\mathbf{G}^{\perp} = \mathbf{G}_1^{\perp} \cap \mathbf{G}_0^{\perp}$ and $\mathbf{G}_0$ is a self-orthogonal matrix. Thus, we conclude that $\mathcal{C}_1 \subset \mathcal{C}_2$. Combined with $\mathcal{C}_1 = \mathcal{C}_3$ and $\mathcal{C}_2 = \mathcal{C}_4$, we can get $\mathcal{C}_1/\mathcal{C}_2^{\perp} \subset \mathcal{C}_3 \subset \mathcal{C}_4$. Also, note that $\mathbf{A} = \mathbf{B} = \mathbf{G}_1 \cong \mathcal{C}_1/\mathcal{C}_2^{\perp}$, thus $\mathbf{A}\mathbf{A}^T = \mathbf{G}_1\mathbf{G}_1^T$. As $\mathbf{G}_1$ is part of a triorthogonal matrix with all odd rows, we have $\mathbf{G}_1\mathbf{G}_1^T = \mathbf{I}$. It follows that all the constraints in (9) are satisfied. □

The CZ-transversality removes the need to implement CZ through CCZ, allowing for a more efficient logical Hadamard gate implementation. The protocol is depicted in Fig. 2, and is described as follows:

- An arbitrary logical code state $|\psi\rangle_L$ is used as input.
- An ancilla block is prepared in $|+\rangle_L$ state.
- Transversal CZ gates are applied to n pairs of physical qubits between $|\psi\rangle_L$ and $|+\rangle_L$.
- A logical $\mathbf{X}$-base measurement is performed on the data block.
- Based on the measurement outcome, a logical Pauli $\mathbf{X}$ operation is applied to the ancilla block. The final state in ancilla block is $\mathbf{H}|\psi\rangle_L$, completing the logical Hadamard gate.

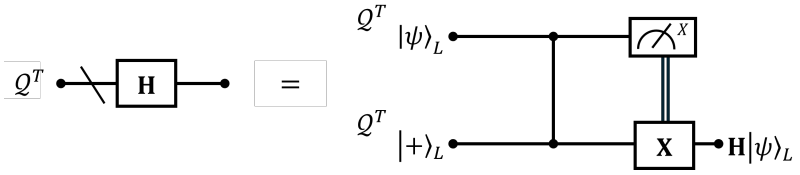

Figure 2: The triorthogonal code logical Hadamard gate circuit with an ancilla block. The logical CZ gate can be applied transversally since $\mathcal{Q}^T$ satisfies (9).

4 Transversal Code Switching

According to the Eastin-Knill theorem, no QECC can support a universal transversal gate set [6]. However, this does not prevent one from using multiple codes within a system to form a universal gate set. Specifically, if one code admits transversal non-Clifford gates and another supports transversal Clifford gates, then by teleporting logical information between them, a universal gate set can be implemented using only transversal operations within each code [12, 23].

For practical implementation of the above approach, we suggest taking an $[[n, k, d]]$ T-triorthogonal code $\mathcal{Q}^T$ and finding a symmetric CSS code $\mathcal{Q}^{\mathrm{Sym}}$ such that these two codes form a code pair satisfying conditions (9) and (6), i.e., being CNOT and CZ-transversal.

Unlike former code switching approaches in [12, 23], our method deterministically teleports logical states between $\mathcal{Q}^T$ and $\mathcal{Q}^{\mathrm{Sym}}$ using transversal state teleportation circuits. This enables the desired logical operations to be implemented transversally throughout the process. We refer to this method as *transversal code switching*. A related method was recently proposed in [15], where the authors perform transversal code switching between 2D and 3D color codes using one-way transversal CNOT gates. Our method could be applied to any T-triorthogonal code $\mathcal{Q}^T$ and proposes a systematic construction of symmetric CSS code $\mathcal{Q}^{\mathrm{Sym}}$. Moreover, it can be integrated into the Steane error correction procedure without incurring additional overhead. We will demonstrate how this can be done in Sec. 5.

4.1 Symmetric Code Generation

For achieving universal computations, we need to find a symmetric code $\mathcal{Q}^{\mathrm{Sym}}$ to pair with a T-triorthogonal code $\mathcal{Q}^T$. In addition, for fault-tolerant state teleportation, the pair $\mathcal{Q}^T$ and $\mathcal{Q}^{\mathrm{Sym}}$ of codes have to support CNOT and CZ-transversality, i.e., they have to satisfy (6) and (9). Here, we generate $\mathcal{Q}^{\mathrm{Sym}}$ from $\mathcal{Q}^T$ in a systematic way. First note that any symmetric code is Hadamard transversal. Therefore CNOT-transversality implies CZ-transversality, hence it is sufficient to construct $\mathcal{Q}^{\mathrm{Sym}}$ satisfying (6).

Lemma 1. *Let $\mathcal{Q}^T = \mathrm{CSS}(\mathcal{C}_1, \mathcal{C}_2)$ be a T-triorthogonal $[[n, k, d]]$ code, and let $\mathcal{C}$ be such that $\mathcal{C}_1 \subset \mathcal{C} \subset \mathcal{C}_2$. Then $\mathcal{Q}^T$ and the symmetric $[[n, k, d']]$ CSS code $\mathcal{Q}^{\mathrm{Sym}} = \mathrm{CSS}(\mathcal{C}, \mathcal{C})$ form a CNOT-transversal code pair, and $d' \geq d$.*

Proof. Since $\mathcal{C}_1 \subset \mathcal{C} \subset \mathcal{C}_2$, the generator matrix of $\mathcal{C}$ can be written as

$$\mathbf{G}_{\mathcal{C}} = \begin{bmatrix} \mathbf{G} \\ \mathbf{B} \end{bmatrix} = \begin{bmatrix} \mathbf{G}_1 \\ \mathbf{G}_0 \\ \mathbf{B} \end{bmatrix}, \tag{14}$$

where $\mathbf{G}$ is a triorthogonal matrix (12), and $\mathbf{B}$ is a submatrix of $\mathbf{G}_0^{\perp}$. Since $\mathcal{C}_2^{\perp} \subset \mathcal{C}^{\perp} \subset \mathcal{C}_1^{\perp}$,

we can write the parity check matrix of $\mathcal{C}$, $\mathbf{G}_{\mathcal{C}}^{\perp}$, as follows

$$\mathbf{G}_{\mathcal{C}}^{\perp} = \begin{bmatrix} \mathbf{G}_0 \\ \mathbf{D} \end{bmatrix}. \tag{15}$$

The restriction $\mathcal{C}^{\perp} \subset \mathcal{C}$ of symmetric CSS codes implies that $\mathbf{G}_{\mathcal{C}}^{\perp}$ should be a self-orthogonal matrix. As $\mathbf{G}_1$ is not self-orthogonal, $\mathbf{D}$ has to be a submatrix of $\mathbf{B}$. According to the definition of the CSS code we have $|\mathcal{C}|/|\mathcal{C}^{\perp}| = 2^k$. Since the number of rows of $\mathbf{G}_1$ is k, we conclude that $\mathbf{D} = \mathbf{B}$.

Thus $\mathcal{C}_1/\mathcal{C}_2^{\perp} \cong \mathbf{G}_1$ and $\mathcal{C}/\mathcal{C}^{\perp} \cong \mathbf{G}_{\mathcal{C}}/\mathbf{G}_{\mathcal{C}}^{\perp} = \mathbf{G}_1$. So $\mathcal{C}_1/\mathcal{C}_2^{\perp} \cong \mathcal{C}/\mathcal{C}^{\perp}$ and $\mathcal{C}_2^{\perp} \subset \mathcal{C}^{\perp}$, the codes fulfill the CNOT transversality conditions (6). We thus have a transversal CNOT gate from $\mathcal{Q}^T$ (control) to $\mathcal{Q}^{\mathrm{Sym}}$ (target). Since $\mathcal{C} \subset \mathcal{C}_2$ and $\mathcal{C}_1/\mathcal{C}_2^{\perp} \subset \mathcal{C}$, we also have CZ transversality.

The code distance of a $\mathrm{CSS}(\mathcal{C}_{\mathrm{i}}, \mathcal{C}_{\mathrm{j}})$ code is $d = \min(d_i, d_j^{\perp})$, where d_i and d_j are the code distances of binary spaces $\mathcal{C}_i/\mathcal{C}_j^{\perp}$ and $\mathcal{C}_j/\mathcal{C}_i^{\perp}$. We already showed that $\mathcal{C}_1/\mathcal{C}_2^{\perp} \cong \mathcal{C}/\mathcal{C}^{\perp}$ which indicates that $d_1 = d'$. For a symmetric code with distance d', we have $d = \min(d', d_2)$, accordingly we have $d \leq d'$. □

Theorem 2. *For any T-transversal CSS code* $[[n, k, d]]$ $\mathcal{Q}^T$ *with* $n - k = 0 \bmod 2$*, there exists a symmetric code* $\mathcal{Q}^{\mathrm{Sym}} = \mathrm{CSS}(\mathcal{C}, \mathcal{C})$ *such that the pair is CNOT-transversal.*

Proof. Based on Lemma 1, to construct $\mathcal{Q}^{\mathrm{Sym}}$ from $\mathcal{Q}^T$, we need to find a self-orthogonal matrix $\mathbf{B}$ which is a submatrix of $\mathbf{G}_0^{\perp}$. Since the dimension of $\mathbf{G}_{\mathcal{C}}^{\perp}$ is $\frac{n-k}{2}$, the dimension of $\mathbf{B}$ is $\frac{n-k-2m}{2} \times n$, where m is the number of rows in $\mathbf{G}_0$. As $\mathcal{C}_2^{\perp} \subset \mathcal{C}_1^{\perp}$ implies $m < n-m-k$, it follows that for any T-triorthogonal code with $n-k = 0 \mod 2$, there exists a symmetric CSS code that satisfies the CNOT transversality conditions. □

As stated in Lemma 1, to construct the symmetric code $\mathcal{Q}^{\mathrm{Sym}}$ from $\mathcal{Q}^T$, we just need to select a full-rank matrix $\mathbf{B}$ which is a submatrix of $\mathbf{G}_0^{\perp}$ with dimension $\frac{n-k-2m}{2} \times n$.

Here we give an example of the $[[15, 1, 3]]$ T-triorthogonal code and the corresponding $\mathcal{Q}^{\mathrm{Sym}}$ code:

Example 1. *The matrices*

$$\mathbf{G} = \left[\frac{\mathbf{G}_0}{\mathbf{G}_1}\right] = \left[\begin{array}{cccccccccccccc} 1&1&1&1&1&1&1&1&0&0&0&0&0&0&0 \\ 1&1&1&1&0&0&0&0&1&1&1&1&0&0&0 \\ 1&1&0&0&1&1&0&0&1&1&0&0&1&1&0 \\ 1&0&1&0&1&0&1&0&1&0&1&0&1&0&1 \\ \hline 1&0&0&1&0&1&1&0&0&1&1&0&1&0&0 \end{array}\right]$$

$$\mathbf{G}_3 = \left[\frac{\mathbf{G}}{\mathbf{B}}\right] = \left[\begin{array}{cccccccccccccc} 1&1&1&1&1&1&1&1&0&0&0&0&0&0&0 \\ 1&1&1&1&0&0&0&0&1&1&1&1&0&0&0 \\ 1&1&0&0&1&1&0&0&1&1&0&0&1&1&0 \\ 1&0&1&0&1&0&1&0&1&0&1&0&1&0&1 \\ 1&0&0&1&0&1&1&0&0&1&1&0&1&0&0 \\ \hline 0&1&1&0&1&0&0&1&0&0&0&0&0&0&0 \\ 0&0&0&0&0&0&0&0&1&0&1&0&0&1&0 \\ 0&0&0&0&0&0&0&0&1&1&0&0&0&0&1 \end{array}\right]$$

define independent stabilizers of a $[[15, 1, 3]]$ *T-triorthogonal code* $\mathcal{Q}^T = \mathrm{CSS}(\mathcal{C}_1, \mathcal{C}_2)$ *and the corresponding symmetric code* $\mathcal{Q}^{\mathrm{Sym}} = \mathrm{CSS}(\mathcal{C}_3, \mathcal{C}_3)$*. Note that matrix* $\mathbf{B}$ *corresponds to*

the selected self-orthogonal matrix in (14)*. The code* $\mathcal{C}_1$*,* $\mathcal{C}_2$ *and* $\mathcal{C}_3$ *are classical linear codes with parameters* $[15, 5, 7]$*,* $[15, 11, 3]$ *and* $[15, 8, 3]$*, respectively. It is important to note that the choice of* $\mathcal{C}_3$ *is not unique. In this example, we can find at least 8 valid alternatives* $\mathcal{C}_3'$ *with the same parameters of* $\mathcal{C}_3$*. Another possible generator matrix is shown below:*

$$\mathbf{G}_3' = \left[\frac{\mathbf{G}}{\mathbf{B}'}\right] = \left[\begin{array}{cccccccccccccc} 1&1&1&1&1&1&1&1&0&0&0&0&0&0&0 \\ 1&1&1&1&0&0&0&0&1&1&1&1&0&0&0 \\ 1&1&0&0&1&1&0&0&1&1&0&0&1&1&0 \\ 1&0&1&0&1&0&1&0&1&0&1&0&1&0&1 \\ 1&0&0&1&0&1&1&0&0&1&1&0&1&0&0 \\ \hline 1&1&0&0&0&0&0&0&1&1&0&0&0&0&0 \\ 0&1&1&0&0&0&0&0&0&1&1&0&0&0&0 \\ 0&0&1&1&0&0&0&0&0&0&1&1&0&0&0 \end{array}\right].$$

The possibility of choosing $\mathcal{C}_3$ *in a multiple possible ways can be important for practical realization of code switching. More detailed studies of the different options will be conducted in future work. All the details about stabilizer generators of each code are listed in App. A.*

4.2 State Teleportation Circuits

In this section, we present circuits that enable logical state teleportation between $\mathcal{Q}^T$ and $\mathcal{Q}^{\text{Sym}}$, facilitating dynamic code switching during computations. The teleportation circuit from $\mathcal{Q}^T$ to $\mathcal{Q}^{\text{Sym}}$ is shown in Fig. 3 (a). It works as follows:

- The input data block is encoded in $\mathcal{Q}^T$ with an arbitrary state $|\psi\rangle_L$.
- An ancilla block is prepared in the $|0\rangle_L$ state, encoded with $\mathcal{Q}^{\text{Sym}}$.
- A transversal CNOT gate is applied between corresponding n physical qubits of $\mathcal{Q}^T$ (control) and $\mathcal{Q}^{\text{Sym}}$ (target).
- A logical $\mathbf{X}$-basis measurement is performed on the data block $\mathcal{Q}^T$.
- Based on the measurement outcome, a logical Pauli $\mathbf{Z}$ operation is applied to the ancilla block. The resulting state in $\mathcal{Q}^{\text{Sym}}$ is $|\psi\rangle_L$, completing the logical state transfer.

The reverse teleportation, from $\mathcal{Q}^{\text{Sym}}$ to $\mathcal{Q}^T$, cannot be achieved using the same circuit, as the logical CNOT in that direction is not transversal. Instead, we use the transversal logical CZ gate between these two codes. The corresponding teleportation circuit is shown in Fig. 3(b), and the procedure is as follows:

- The input data block is encoded in $\mathcal{Q}^{\text{Sym}}$ with an arbitrary state $|\psi\rangle_L$.
- An ancilla block is prepared in the logical $|+\rangle_L$ state, encoded with $\mathcal{Q}^T$.
- Transversal logical Hadamard gates are applied to the data block.
- Transversal CZ gate is applied between $\mathcal{Q}^{\text{Sym}}$ and $\mathcal{Q}^T$.
- A logical $\mathbf{X}$-base measurement is performed on the data block $\mathcal{Q}^{\text{Sym}}$. Based on the measurement outcome, a logical Pauli $\mathbf{X}$ operation is applied to $\mathcal{Q}^T$.
- The final state in $\mathcal{Q}^T$ is $|\psi\rangle_L$, completing the logical teleportation.

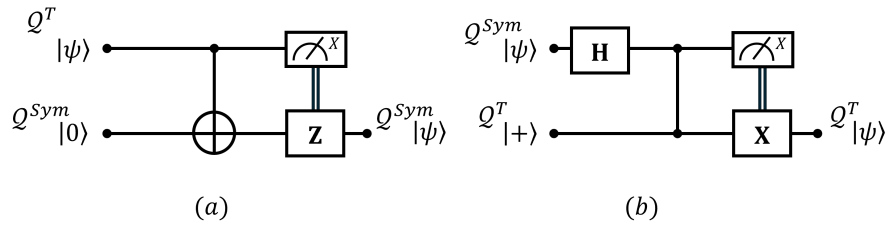

Figure 3: The state teleportation circuits between $\mathcal{Q}^T$ and $\mathcal{Q}^{\text{Sym}}$. (a) The state teleportation from $\mathcal{Q}^T$ to $\mathcal{Q}^{\text{Sym}}$. (b) Since the CNOT gate from $\mathcal{Q}^{\text{Sym}}$ to $\mathcal{Q}^T$ is not transversal, we can use CZ gate instead. The teleportation circuit is similar to Fig.2, but with additional logical Hadamard gate at beginning, and this logical Hadamard gate can be applied transversally on $\mathcal{Q}^{\text{Sym}}$.

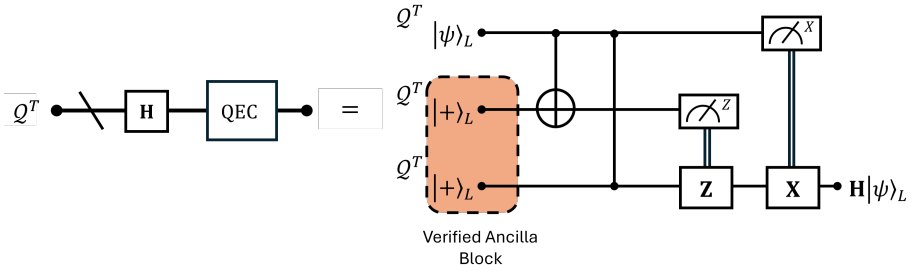

Figure 4: Integration of T-triorthogonal logical Hadamard gate circuit to Steane syndrome extraction. The ancilla blocks are prepared in logical $|+\rangle_L$ states and go through a verification procedure to eliminate high-weight errors.

With these two circuits, we obtain a two-way teleportation between $\mathcal{Q}^T$ and $\mathcal{Q}^{\text{Sym}}$. During computation, logical states can be stored in $\mathcal{Q}^{\text{Sym}}$ while Clifford operations are executed transversally. When non-Clifford gates are required, the logical state is teleported back to $\mathcal{Q}^T$, where such operations can also be applied transversally.

Although each teleportation circuit requires one ancilla code block, this overhead can be reduced by integrating the teleportation procedure into the Steane syndrome extraction process. We provide more details on this in the following section.

5 Steane Error Correction Circuit

In this section, we show how to merge two methods proposed in this paper into Steane error correction procedure.

To implement a fault-tolerant logical Hadamard gate, we integrate the operation into the Steane syndrome extraction circuit, as shown in Fig.4. Both data and ancilla blocks are encoded in the same T-triorthogonal code $\mathcal{Q}^T$. Two ancilla blocks are prepared in logical $|+\rangle_L$ state, and verified to suppress high-weight errors. The first ancilla block is used for Pauli **X** error detection, via transversal CNOT gates from the data block. Any physical Pauli **X** errors in the data block propagate to the ancilla and can be identified by performing **Z**-base measurements on the ancilla qubits. The second ancilla block is then coupled to the data block via transversal CZ gates, followed by a full **X**-base measurement on all data qubits.

The initial **Z**-base measurements yield error syndromes that can identify and correct physical **X** errors with weight up to $\lfloor \frac{d}{2} \rfloor$, where d is the code distance. However, since the transversal CZ gate is applied after the CNOT operation, any **X** errors on the data block propagate to the second ancilla block as Pauli **Z** errors. Therefore, recovery operations

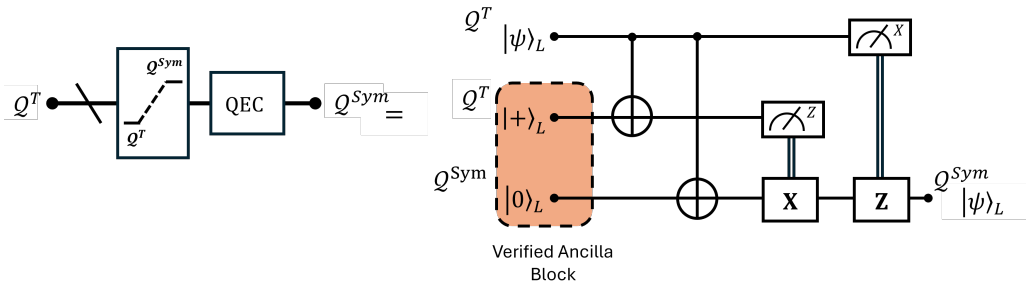

Figure 5: The state teleportation circuit from $\mathcal{Q}^T$ to $\mathcal{Q}^{\mathrm{Sym}}$, embedded with Steane syndrome extraction procedure. After the circuit is executed, the logical state is re-encoded in $\mathcal{Q}^{\mathrm{Sym}}$, and one round of error correction has been completed.

must be applied to the second ancilla block, incorporating a basis change from Pauli **X** to **Z**.

The **X**-base measurements on the data block yield a classical binary vector corresponding to a (possibly corrupted) codeword in $\mathcal{C}_2$. Using the extracted syndrome, **Z** errors on the data can be identified and corrected. Since **Z** errors commute with the CZ gates, they do not propagate to the second ancilla block, which stores in the data block. After correction, the resulting binary vector is projected back into $\mathcal{C}_2$, and the logical Pauli **X** operator is used to determine whether the logical state is $|+\rangle_L$ or $|-\rangle_L$. If the result is $|-\rangle_L$ state, a logical **X** operator is applied as feedback. This protocol ensures that any $t < \lfloor \frac{d}{2} \rfloor$ physical errors will result in at most t errors in the final logical state, thereby preserving the fault-tolerant threshold.

As discussed previously, the logical state teleportation circuits from $\mathcal{Q}^T$ to $\mathcal{Q}^{\mathrm{Sym}}$ shown in Fig. 3(a) can be embedded into the syndrome extraction process in a manner that preserves fault-tolerance. The teleportation circuit in Fig. 3(a), merged with Steane error correction procedure is shown in Fig. 5. The circuit on the right represents the process in which the logical state, initially encoded in $\mathcal{Q}^T$ is teleported into $\mathcal{Q}^{\mathrm{Sym}}$ while simultaneously performing one round of error correction. Similarly, the merged version of the circuit in Fig. 3(b) is shown in Fig. 6, where the logical state is teleported from $\mathcal{Q}^{\mathrm{Sym}}$ to $\mathcal{Q}^T$, followed by a round of error correction.

After integration into the Steane error correction procedure, both the CZ-based logical Hadamard method from section 3 and transversal code switching method from Sec. 4 require comparable overhead. In scenarios where Hadamard and non-Clifford gates are interleaved, such as in a gate sequence like $-\mathbf{T}-\mathbf{H}-\mathbf{T}-$, the direct Hadamard implementation implementation is more efficient, as code switching must be applied twice per operation in the alternative approach. However, in scenarios involving frequent Clifford operations, the code switching method offers greater flexibility. For instance, in high physical-fidelity regimes, error correction can be applied less frequently, making this method potentially more resource efficient. Also, compared with the logical Hadamard method, transversal code switching is natively more effective for managing non-local errors if universal distributed quantum computing is realized using 2G quantum communication, see [18].

6 Qubit Resource Estimation

In this section, we compare the resource cost of our proposed protocols with those of previously reported methods [11, 15, 17], using the number of qubits and quantum gates as key metrics. Taking the 15-qubit code, which is the smallest distance-3 T-triorthogonal

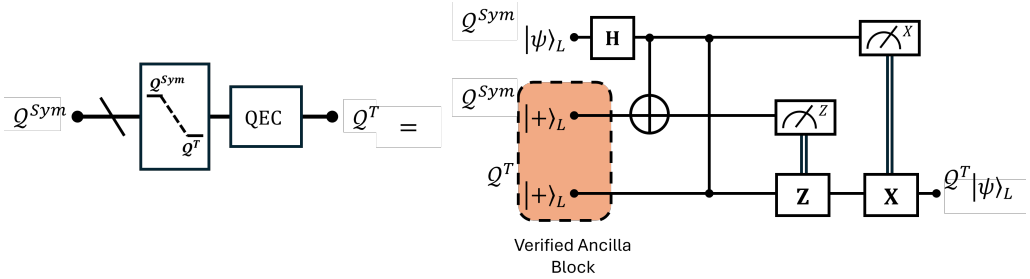

Figure 6: The state teleportation circuit from $\mathcal{Q}^{\mathrm{Sym}}$ to $\mathcal{Q}^{T}$, embedded with Steane syndrome extraction procedure. After the circuit is executed, the logical state is re-encoded in $\mathcal{Q}^{T}$, and one round of error correction has been simultaneously completed.

code [24] as an example, we explicitly calculate and analyze the resource requirements for each protocol.

6.1 Logical Hadamard Gate Protocols

First, we analyze the logical Hadamard gate using the CZ-based protocol (see Fig. 2) and compare it with the logical Hadamard protocol proposed in [11]. Since both protocols allow integration into the Steane error correction framework, the protocols require the same number of resources: two ancilla blocks which means additional 30 ancilla qubits and 30 CNOT (or equivalently CZ) gates, neglecting the cost of fault-tolerant state preparation.

However, our protocol, in contrast to the one from [11], does not compromise the error correction ability of the code. Below we show that in the case of 15-qubit code our protocol allows correction three time more X-errors than the protocol form [11].

To see this, we compare the logical error rate after a full round of error correction. In the protocol of [11], transversal physical Hadamard gates are applied to the data qubits, followed by an X-error correction procedure. However, the physical Hadamard operation does not preserve the code space, thereby reducing the effectiveness of the subsequent X-error correction procedure. For the 15-qubit code, the X-error correction procedure can ideally correct up to three Pauli-X errors. After applying transversal Hadamard gates, some of the Z-stabilizers must instead be used to project the state back into the code space, reducing the correction capacity to only one Pauli-X error. The capability to correct Pauli-Z errors remains limited to one. Let us consider the following physical qubit error model:

$$\mathcal{N}(\boldsymbol{\rho}) = (1-2p)\boldsymbol{\rho} + p\mathbf{X}\boldsymbol{\rho}\mathbf{X} + p\mathbf{Z}\boldsymbol{\rho}\mathbf{Z}\,.$$

As there are now $2 \times \binom{15}{2} = 210$ uncorrectable weight-2 errors, the logical error rate after a complete round of X- and Z-error correction is $210\,p^2 + O(p^3)$.

In the CZ-based logical Hadamard gate protocol of Section 3, Pauli-X errors are detected and corrected using the first ancilla block. Assuming the logical ancilla states are verified and error-free, Pauli-X errors on the data qubits propagate as X errors to the first ancilla and as Z errors to the second ancilla. Recovery Z operations are then applied to the second ancilla block, allowing up to three Pauli-X errors to be corrected in the data block. Since the data block is measured in the logical X basis, any Pauli-Z errors in the data blocks directly affect the outcome. For the 15-qubit code, single-qubit Z errors can still be corrected. Under the same noise model, the resulting logical error rate for our protocol is $105\,p^2 + O(p^3)$, which is a factor of two improvement over the previous approach.

Methods	No State Prep.				With State Prep.			
	Qubits		Gates		Qubits		Gates	
Our method	45	45	30	30	48	48	96	96
Flag switching [17]	17	18	174	204	17	18	174	204
Transversal [15] Flag	24	25	43	139	25	26	54	197
Transversal [15] Steane	36	52	21	37	38	57	54	211

Table 1: We compare the total resource cost, both in terms of qubits and two-qubit gates. The first value in each block indicates the cost of performing code switching from the $[[15, 1, 3]]$ code to the Steane code (or Symmetric code in our method) along with one round of error correction. The second value indicates the cost for reverse switching. Our method has the same cost in both directions. The comparison is made both with and without the cost of logical state preparation. "Transversal flag" and "Transversal Steane" refer to the use of the flag-based fault-tolerant and Steane error correction methods, respectively. For the flag-based code-switching protocol [17], the resource requirements remain the same with or without state preparation, as no additional ancilla block is prepared in this method.

6.2 Transversal Code Switching

In this section, we evaluate the resource cost of performing code switching together with one full round of error correction, and compare the total overhead of our deterministic method with prior art protocols. In Table 1, we show the different cost for three protocols - the transversal codes witching method of Section 4, the deterministic fault-tolerant code switching protocol of [17], and the recently proposed transversal code switching protocol of [15].

The comparison is performed under two scenarios. In the first, the ancilla states are assumed to be pre-prepared, and the corresponding preparation cost is not included. In the second, a more comprehensive scenario is considered, where ancilla states are prepared when needed, and their preparation cost is included in the total resource estimate. Based on the special structural correlation between the two switched codes, we propose a modified state preparation method using flag qubits, which significantly reduces both gate and qubit overhead compared with the conventional Steane's error correction approach. In the following, we explain how to find the corresponding costs given in the Table 1 for our scheme.

6.2.1 Cost without State Preparation

In transversal code switching protocols, ancilla block are initialized in logical $|0\rangle_L$ or $|+\rangle_L$ states. The preparation of these states can be resource-intensive, but it can also be performed in advance so that the ancilla blocks are ready for use when required. Therefore, in the first part of our analysis, we neglect the cost of ancilla state preparation and assume that these states are pre-prepared and readily available.

The deterministic code switching protocol introduced in [17] employs two flag qubits to maintain fault tolerance during transitions between the $[[7, 1, 3]]$ Steane code and the $[[15, 1, 3]]$ triorthogonal code. To ensure fault-tolerant switching, a large number of CNOT gates are necessary. Specifically, to prevent high-weight Pauli-X errors that may arise during ancilla preparation, a round of X-error correction on the triorthogonal code must be performed before switching from the triorthogonal to the Steane code. Switching from the Steane code to the triorthogonal code requires 72 CNOT gates, while a round of X-error correction procedure with flag-qubit fault tolerance requires 120 additional CNOT gates. The reverse switching, from the triorthogonal code back to the Steane code, requires 18

CNOT gates. Following the switching process, a full round of error correction is performed using the flag-qubit error correction method. Depending on the final code, this step requires either 3 ancilla qubits and 132 CNOT gates (for the Steane code) or 2 ancilla qubits and 36 CNOT gates (for the triorthogonal code) [25, 26]. In total, the resource cost for the combined code switching and error correction procedure is 17 qubits and 174 CNOT gates when switching from the triorthogonal to the Steane code, and 18 qubits and 204 CNOT gates for the reverse direction.

Another transversal code-switching method was recently proposed in [15]. In this work, the authors demonstrate code switching between a two-dimensional color code (the Steane code) and a three-dimensional color code (the tetrahedral code) using one-way transversal CNOT gates. Excluding the cost of state preparation, their method requires 22 qubits and 7 CNOT gates to switch from one code to the other. After the switching, an additional round of error correction is performed on the Steane code, requiring 2 ancilla qubits and 36 CNOT gates, or on the tetrahedral code, requiring 3 ancilla qubits and 132 CNOT gates, both implemented using flag-qubit fault-tolerant techniques. The total resource cost for the complete procedure is therefore 24 qubits with 42 CNOT gates when switching from the tetrahedral to the Steane code, and 25 qubits with 139 CNOT gates for the reverse direction. Alternatively, when Steane's error correction framework is employed, the total resource cost is 36 qubits (22 qubits if fast-rest in the physical qubits is available) with 21 CNOT gates for the Steane code, and 52 qubits with 37 CNOT gates for the tetrahedral code.

In our code-switching procedure, transversal CNOT or CZ gates are used to teleport the logical state from the data block to an encoded ancilla block. This step requires only an additional 15 qubits and 15 CNOT (or CZ) gates. Since our protocol can be seamlessly integrated into the Steane error correction framework, we adopt Steane's method for the subsequent error correction process. As illustrated in Fig. 5 and Fig. 6, two ancilla blocks are prepared and verified in the logical $|+\rangle_L$ and $|0\rangle_L$ states. Transversal CNOT gates are then applied, followed by measurements on all physical qubits, teleporting the logical state from one code to the other. This procedure is fault-tolerant, as all operations are transversal and the $2n$ physical qubits in data and the first ancilla block are measured simultaneously at the end of the circuit. Any single-qubit error occurring during the process can propagate to at most one single-qubit error in the final logical state. Neglecting the cost of logical state preparation, the total resources required to complete both code switching and error correction are three ancilla blocks and two sets of transversal two-qubit gates. For the 15-qubit code, this corresponds to 45 qubits and 30 two-qubit gates.

Comparing with the flag based methods, our protocol requires a higher qubit overhead but significantly fewer gates. Comparing to using Steane method for [15], our protocol requires comparable numbers of qubits and gates. In regimes with relatively high gate error rates, this reduction in gate operations should lead to better overall performance. Furthermore, unlike codes used in [15], our codes $\mathcal{Q}^T$ and $\mathcal{Q}^{\mathrm{Sym}}$ are simultaneously both CNOT and CZ transversal. This means that frequent code switching is unnecessary. This property enables additional circuit-level optimization, where the transversality can be exploited to minimize the number of switching operations required throughout computation.

6.2.2 Cost with State Preparation

In this section, we take into account the resource cost associated with logical state preparation. We first briefly review the state preparation methods used in other protocols and analyze their corresponding resource requirements. Building on the special correlation between the two switching codes, we then propose a new fault-tolerant state preparation

method integrated with our transversal code-switching protocol, which effectively reduces the overall gate overhead. The resource costs for all protocols are summarized in Table 1.

Since the logical state is switched between different codes, fault-tolerant ancilla state preparation imposes additional requirements compared with conventional methods [21, 27]. Errors that are correctable in one code may become uncorrectable, and cause a logical error, after switching to another code. In particular, high-weight Pauli-X errors that are correctable within the triorthogonal code can propagate into logical errors once the state is mapped to the Steane code, which has a smaller code distance. Therefore, an additional round of X-error correction must be performed before switching from the $[[15, 1, 3]]$ code to Steane code [17].

In the method proposed in [15], the 15-qubit ancilla state also requires the removal of high-weight X-errors. Instead of performing an additional round of X-error correction, the authors measure a subset of the Z-stabilizer generators to eliminate these high-weight errors. Using their approach, the non–fault-tolerant preparation of the $|+\rangle_L$ state in the 15-qubit code requires 15 qubits and 25 CNOT gates. The subsequent verification procedure adds 5 additional ancilla qubits (one with fast-reset qubit) and 33 CNOT gates, resulting in a total of 20 qubits and 58 CNOT gates. For the Steane code, the corresponding preparation requires 8 qubits and 11 CNOT gates.

In our method, the symmetric code generated from the T-triorthogonal code has a lower capacity for correcting Pauli-X errors, since Z-stabilizer group of the symmetric code is a subset of that of the T-triorthogonal code $\mathcal{C}_3^{\perp} \subset \mathcal{C}_1^{\perp}$, while both codes have the same code distance for Pauli-Z errors. Therefore, it is essential to ensure that high-weight Pauli-X errors do not induce logical errors after switching from $\mathcal{Q}^T$ to $\mathcal{Q}^{\mathrm{Sym}}$. As shown in Fig. 5, the first ancilla block is prepared in $|+\rangle_L$ using $\mathcal{Q}^T$ code.The standard fault-tolerant state verification procedure guarantees that a single Pauli-Z error does not produce a logical Z error and therefore does not flip the logical state from $|+\rangle_L$ to $|-\rangle_L$. However, high-weight X error that are not detected during verification can still occur, potentially leading to nontrivial syndromes during Z-basis measurement. After applying the corresponding recovery X operations in $\mathcal{Q}^{\mathrm{Sym}}$, these high-weight X errors may be mapped into the symmetric code and cause logical errors. It is worth noting that because $\mathcal{Q}^T$ and $\mathcal{Q}^{\mathrm{Sym}}$ share a subset of common Z-stabilizer generators, the symmetric code retains partial capability to correct such high-weight Pauli-X errors. Consider an error vector $\mathbf{e} = \mathbf{D}(\mathbf{a_e}, \mathbf{0})$ that occurs in $\mathcal{Q}^T$ and flips only the overlapping Z-stabilizer generators flipping. This error leads to a recovery operation $\mathbf{R} = \mathbf{D}(\mathbf{a_R}, \mathbf{0})$ that restores the stabilizer outcomes. Upon switching, this recovery operation is mapped into $\mathcal{Q}^{\mathrm{Sym}}$ as $\mathbf{D}(\mathbf{0}, \mathbf{a_R})$. Since $\mathcal{Q}^{\mathrm{Sym}}$ has identical X- and Z-stabilizer generators, the error vector $\mathbf{D}(\mathbf{a_R}, \mathbf{0})$ that is correctable under X-error correction in $\mathcal{Q}^T$ corresponds to $\mathbf{D}(\mathbf{0}, \mathbf{a_R})$, which is likewise correctable under Z-error correction in $\mathcal{Q}^{\mathrm{Sym}}$.

Owing to this property, an additional step can be incorporated into the verification procedure, in which only the stabilizer generators that are excluded from $\mathcal{Q}^{\mathrm{Sym}}$ are measured. The prepared state is accepted only if all measured syndromes are trivial; otherwise, the state is discarded and the preparation process is restarted. This additional verification step ensures that the remaining high-weight X errors can be detected and subsequently corrected by $\mathcal{Q}^{\mathrm{Sym}}$. The verification circuit for the code presented in Example. 1 is shown in App. B

The conventional fault-tolerant preparation of $|+\rangle_L$ state in $\mathcal{Q}^T$ requires 16 qubits (15 data qubits and 1 ancilla) and 32 CNOT gates [25, 17]. Our additional verification step introduces 2 ancilla qubits (or 1 ancilla if a fast-reset qubit is available) and 12 CNOT gates [28]. In total, the verified state preparation procedure requires 17 qubits

and 44 CNOT gates for preparing $|+\rangle_L$ state in $\mathcal{Q}^T$. For the state preparation of $\mathcal{Q}^{\text{Sym}}$, a non–fault-tolerant encoding circuit followed by a verification procedure can be used. This approach requires 16 qubits and 22 CNOT gates [29, 30]. The corresponding state preparation circuit is shown in App. B Fig. 8.

The fault-tolerant state preparation can be achieved in different manner. Using the Steane's method shown in Fig. 1, one need three additional blocks with transversal CNOT gates to verify an ancilla block. The overhead is significantly larger than flag qubit fault-tolerant manner.

After considering the extra cost for state preparation, our method significantly reduce the overhead of CNOT gates compare with other methods, due to the exploitation of correlation of structure between two switching codes. In the NISQ system with limited fidelity on two-qubit gates, our method can outperform than others.

7 Conclusion

We have presented two methods to achieve universal fault-tolerant quantum computation using T-triorthogonal codes. The first is an optimized construction of the logical Hadamard gate using the transversal CZ of T-triorthogonal codes, reducing circuit overhead while maintaining fault-tolerance. When combined with **T**-transversality, this results in a universal fault-tolerant scheme for T-triorthogonal codes. The second method introduces a symmetric CSS code generated from a T-triorthogonal code, enabling transversal implementation of all logical operations via state teleportation between the two codes. We provided explicit criteria for constructing the symmetric code, ensuring they meet the conditions for transversal CNOT and CZ gates. Both methods can be generalized to any **T**-transversal triorthogonal code.

Using a 15-qubit T-triorthogonal code as an example, we demonstrated the validity of our approach and constructed teleportation circuits that enable efficient logical state teleportation. Crucially, we showed that both the optimized Hadamard gate and teleportation protocols can be integrated into the Steane error correction framework without requiring additional resource overhead. This integration preserves fault-tolerance and makes our approach practically viable for scalable quantum architectures. Comparing the resource cost of our protocol with those of other methods on the 15-qubit code shows that our approach reduces the overhead of universal quantum computation by minimizing gate and qubit requirements. Future work may investigate generalizations to other code families and explore integration into alternative fault-tolerant frameworks such as Knill's error correction.

References

[1] Michael A Nielsen and Isaac L Chuang. "Quantum computation and quantum information". Cambridge University Press. (2010).

[2] I. L. Chuang and R. Laflamme. "Quantum error correction by coding" (1995). arXiv:quant-ph/9511003.

[3] Raymond Laflamme, Cesar Miquel, Juan Pablo Paz, and Wojciech Hubert Zurek. "Perfect quantum error correction code" (1996). arXiv:quant-ph/9602019.

[4] Daniel Gottesman. "Theory of fault-tolerant quantum computation". Physical Review A **57**, 127–137 (1998).

[5] John Preskill. "Fault-tolerant quantum computation" (1997). arXiv:quant-ph/9712048.

[6] Bryan Eastin and Emanuel Knill. "Restrictions on transversal encoded quantum gate sets". Physical Review Letters **102**, 110502 (2009).

[7] Sergey Bravyi and Alexei Kitaev. "Universal quantum computation with ideal clifford gates and noisy ancillas". Physical Review A **71**, 022316 (2005).
[8] Ying Li. "A magic state's fidelity can be superior to the operations that created it". New Journal of Physics **17**, 023037 (2015).
[9] Austin G Fowler, Simon J Devitt, and Cody Jones. "Surface code implementation of block code state distillation". Scientific reports **3**, 1939 (2013).
[10] Narayanan Rengaswamy, Robert Calderbank, Michael Newman, and Henry D Pfister. "On optimality of CSS codes for transversal T". IEEE Journal on Selected Areas in Information Theory **1**, 499–514 (2020).
[11] Adam Paetznick and Ben W Reichardt. "Universal fault-tolerant quantum computation with only transversal gates and error correction". Physical Review Letters **111**, 090505 (2013).
[12] Jonas T Anderson, Guillaume Duclos-Cianci, and David Poulin. "Fault-tolerant conversion between the Steane and Reed-Muller quantum codes". Physical Review Letters **113**, 080501 (2014).
[13] Theodore J Yoder. "Universal fault-tolerant quantum computation with Bacon-Shor codes" (2017). arXiv:1705.01686.
[14] Darren Banfield and Alastair Kay. "Implementing clifford gates on stabilizer codes via measurement" (2022). arXiv:2210.14074.
[15] Sascha Heußen and Janine Hilder. "Efficient fault-tolerant code switching via one-way transversal CNOT gates". Quantum **9**, 1846 (2025).
[16] Andrew M Steane. "Active stabilization, quantum computation, and quantum state synthesis". Physical Review Letters **78**, 2252 (1997).
[17] Friederike Butt, Sascha Heußen, Manuel Rispler, and Markus Müller. "Fault-tolerant code-switching protocols for near-term quantum processors". PRX Quantum**5** (2024).
[18] Mahdi Bayanifar, Alexei Ashikhmin, Dawei Jiao, and Olav Tirkkonen. "Transversality across two distinct quantum codes and its application to quantum repeaters". In IEEE Internat. Conf. on Quantum Commun., Networking, and Computing (QCNC). Pages 17–23. (2025).
[19] Minjia Shi, Haodong Lu, Jon-Lark Kim, and Patrick Solé. "Triorthogonal codes and self-dual codes". Quantum Information Processing **23**, 280 (2024).
[20] Christopher Chamberland and Pooya Ronagh. "Deep neural decoders for near term fault-tolerant experiments". Quantum Science and Technology **3**, 044002 (2018).
[21] Christopher Chamberland and Michael E. Beverland. "Flag fault-tolerant error correction with arbitrary distance codes". Quantum **2**, 53 (2018).
[22] Hayato Goto. "Minimizing resource overheads for fault-tolerant preparation of encoded states of the steane code". Scientific reports **6**, 19578 (2016).
[23] Christophe Vuillot, Lingling Lao, Ben Criger, Carmen García Almudéver, Koen Bertels, and Barbara M Terhal. "Code deformation and lattice surgery are gauge fixing". New Journal of Physics **21**, 033028 (2019).
[24] Stergios Koutsioumpas, Darren Banfield, and Alastair Kay. "The smallest code with transversal t" (2022). arXiv:2210.14066.
[25] Rui Chao and Ben W Reichardt. "Fault-tolerant quantum computation with few qubits". npj Quantum Information **4**, 42 (2018).
[26] Prithviraj Prabhu and Ben W. Reichardt. "Fault-tolerant syndrome extraction and cat state preparation with fewer qubits". Quantum **7**, 1154 (2023).
[27] Lukas Postler, Sascha Heuβen, Ivan Pogorelov, Manuel Rispler, Thomas Feldker, Michael Meth, Christian D Marciniak, Roman Stricker, Martin Ringbauer, Rainer

Blatt, et al. “Demonstration of fault-tolerant universal quantum gate operations”. Nature **605**, 675–680 (2022).

[28] Andrea Rodriguez-Blanco, Ho Nam Nguyen, and K. Birgitta Whaley. “Fault-tolerant correction-ready encoding of the [[7,1,3]] steane code on a 2d grid” (2025). arXiv:2504.01083.

[29] Robert Wille, Lucas Berent, Tobias Forster, Jagatheesan Kunasaikaran, Kevin Mato, Tom Peham, Nils Quetschlich, Damian Rovara, Aaron Sander, Ludwig Schmid, Daniel Schoenberger, Yannick Stade, and Lukas Burgholzer. “The MQT handbook: A summary of design automation tools and software for quantum computing”. In IEEE International Conference on Quantum Software (QSW). (2024). arXiv:2405.17543.

[30] Andrew M. Steane. “Fast fault-tolerant filtering of quantum codewords” (2004). arXiv:quant-ph/0202036.

A Stabilizer generators of Example. 1

Here we give the full stabilizer generators in Pauli terms of code $\mathcal{Q}^T$ and $\mathcal{Q}^{\text{Sym}}$ we used in Example. 1.

For $[[15, 1, 3]]$ T-triorthogonal code $\mathcal{Q}^T$, we have 4 X-stabilizer and 10 Z-stabilizer generators:

$$\begin{aligned}
\mathbf{S_x^1} &= \mathbf{X_1X_2X_3X_4X_5X_6X_7X_8}, & \mathbf{S_x^2} &= \mathbf{X_1X_2X_3X_4X_9X_{10}X_{11}X_{12}} \\
\mathbf{S_x^3} &= \mathbf{X_1X_2X_5X_6X_9X_{10}X_{13}X_{14}}, & \mathbf{S_x^4} &= \mathbf{X_1X_3X_5X_7X_9X_{11}X_{13}X_{15}} \\
\mathbf{S_z^1} &= \mathbf{Z_1Z_2Z_3Z_4Z_5Z_6Z_7Z_8}, & \mathbf{S_z^2} &= \mathbf{Z_1Z_2Z_3Z_4Z_9Z_{10}Z_{11}Z_{12}} \\
\mathbf{S_z^3} &= \mathbf{Z_1Z_2Z_5Z_6Z_9Z_{10}Z_{13}Z_{14}}, & \mathbf{S_z^4} &= \mathbf{Z_1Z_3Z_5Z_7Z_9Z_{11}Z_{13}Z_{15}} \\
\mathbf{S_z^5} &= \mathbf{Z_1Z_2Z_3Z_4}, & \mathbf{S_z^6} &= \mathbf{Z_1Z_2Z_5Z_6} \\
\mathbf{S_z^7} &= \mathbf{Z_1Z_3Z_5Z_7}, & \mathbf{S_z^8} &= \mathbf{Z_1Z_2Z_9Z_{10}} \\
\mathbf{S_z^9} &= \mathbf{Z_1Z_5Z_9Z_{13}}, & \mathbf{S_z^{10}} &= \mathbf{Z_1Z_3Z_9Z_{11}}.
\end{aligned}$$

The logical operators of T-triorthogonal code are:

$$\mathbf{Z_L} = \mathbf{Z_1Z_2Z_{15}}, \qquad \mathbf{X_L} = \mathbf{X_1X_4X_6X_7X_{10}X_{11}X_{13}}.$$

The weight-7 Pauli-X operator gallows the code to correct up to weight-3 Pauli-X errors. As for Pauli-Z errors, only single-qubit Pauli-Z error can be corrected.

The paired symmetric code $\mathcal{Q}^{\text{Sym}}$ has 7 X-stabilizer and 7 Z-stabilizer generators:

$$\begin{aligned}
\mathbf{S_x^1} &= \mathbf{X_1X_2X_3X_4X_5X_6X_7X_8}, & \mathbf{S_z^1} &= \mathbf{Z_1Z_2Z_3Z_4Z_5Z_6Z_7Z_8}, \\
\mathbf{S_x^2} &= \mathbf{X_1X_2X_3X_4X_9X_{10}X_{11}X_{12}}, & \mathbf{S_z^2} &= \mathbf{Z_1Z_2Z_3Z_4Z_9Z_{10}Z_{11}Z_{12}}, \\
\mathbf{S_x^3} &= \mathbf{X_1X_2X_5X_6X_9X_{10}X_{13}X_{14}}, & \mathbf{S_z^3} &= \mathbf{Z_1Z_2Z_5Z_6Z_9Z_{10}Z_{13}Z_{14}}, \\
\mathbf{S_x^4} &= \mathbf{X_1X_3X_5X_7X_9X_{11}X_{13}X_{15}}, & \mathbf{S_z^4} &= \mathbf{Z_1Z_3Z_5Z_7Z_9Z_{11}Z_{13}Z_{15}}, \\
\mathbf{S_x^5} &= \mathbf{X_1X_2X_3X_4}, & \mathbf{S_z^5} &= \mathbf{Z_1Z_2Z_3Z_4}, \\
\mathbf{S_x^6} &= \mathbf{X_1X_2X_5X_6}, & \mathbf{S_z^6} &= \mathbf{Z_1Z_2Z_5Z_6}, \\
\mathbf{S_x^7} &= \mathbf{X_1X_3X_5X_7}, & \mathbf{S_z^7} &= \mathbf{Z_1Z_3Z_5Z_7}
\end{aligned}$$

The logical operators of symmetric code are:

$$\mathbf{Z_L} = \mathbf{Z_9Z_{10}Z_{15}}, \qquad \mathbf{X_L} = \mathbf{X_9X_{10}X_{15}}.$$

The minimum weight of both logical operators are 3, it shows $\mathcal{Q}^{\text{Sym}}$ can only promise to correct single Pauli-X and Z error.

B The modified state preparation circuit

In this section, we present circuits for T-triorthogonal code $\mathcal{Q}^T$ extra verification procedure and state preparation circuit for $\mathcal{Q}^{\text{Sym}}$.

Fig. 7 illustrates the additional verification procedure described above. Using $[[15, 1, 3]]$ T-triorthogonal code as an example, we demonstrate how this verification is performed. Since the Z-stabilizer generators of $\mathcal{Q}^{\text{Sym}}$ can be regarded as a subgroup of those of $\mathcal{Q}^T$, it is sufficient to measure only the stabilizer generators that belong exclusively to $\mathcal{Q}^T$. This extra verification step ensures that high-weight errors, which are uncorrectable in $\mathcal{Q}^{\text{Sym}}$,

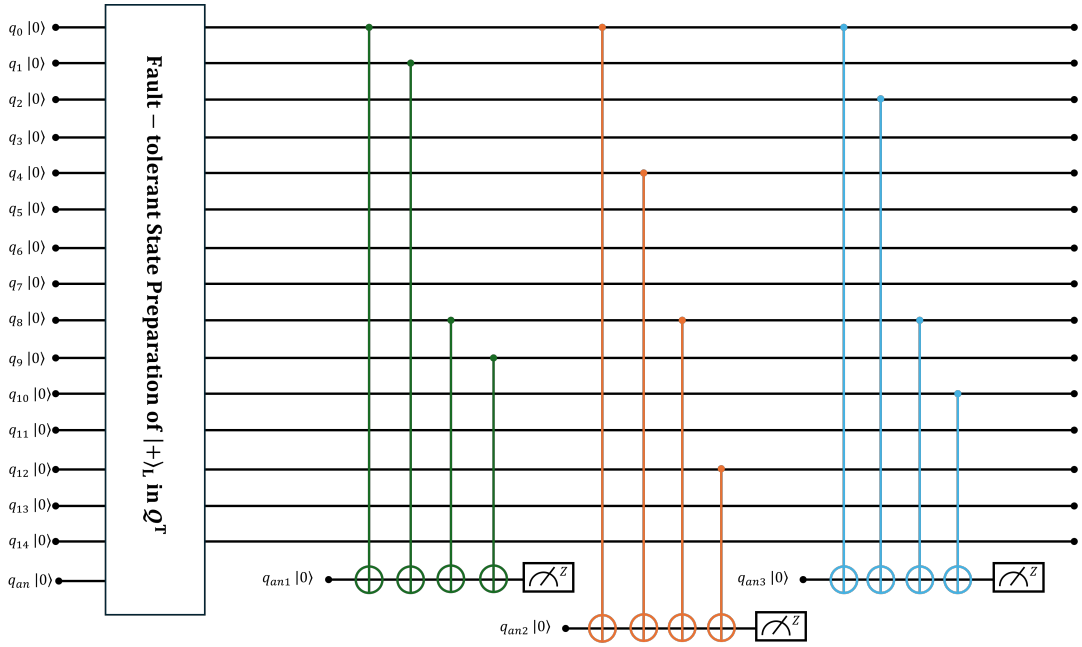

Figure 7: Circuit for additional verification of the $|+\rangle_L$ state in $\mathcal{Q}^T$. The $|+\rangle_L$ state is first prepared and verified in circuit described in [17]. Three additional ancilla qubits are then used for extra verification step, during which the additional stabilizer generators are measured. For $\mathcal{Q}^T$ and $\mathcal{Q}^{\mathrm{Sym}}$ in Example. 1, these extra Z-stabilizer generators correspond to $\mathbf{S_z^8}$, $\mathbf{S_z^9}$ and $\mathbf{S_z^{10}}$, as listed in App. A. The corresponding measurement circuits are shown in green, orange, and blue. If any nontrivial syndrome is detected, the prepared state is discarded and the preparation process is restarted.

are detected and removed. If any nontrivial syndromes are observed, the prepared state is discarded and the entire procedure is restarted from the beginning.

Fig. 8 shows the flag-based fault-tolerant state preparation circuit for $\mathcal{Q}^{\mathrm{Sym}}$. This circuit prepares the logical $|0\rangle_L$ state, using an ancilla qubit to measure the logical Z operator and detect potential high-weight Pauli-X errors. The circuit for preparing the logical $|+\rangle_L$ state follows the same structure, with additional 15 physical Hadamard gates applied at the end to transform the logical $|0\rangle_L$ into logical $|+\rangle_L$ state.

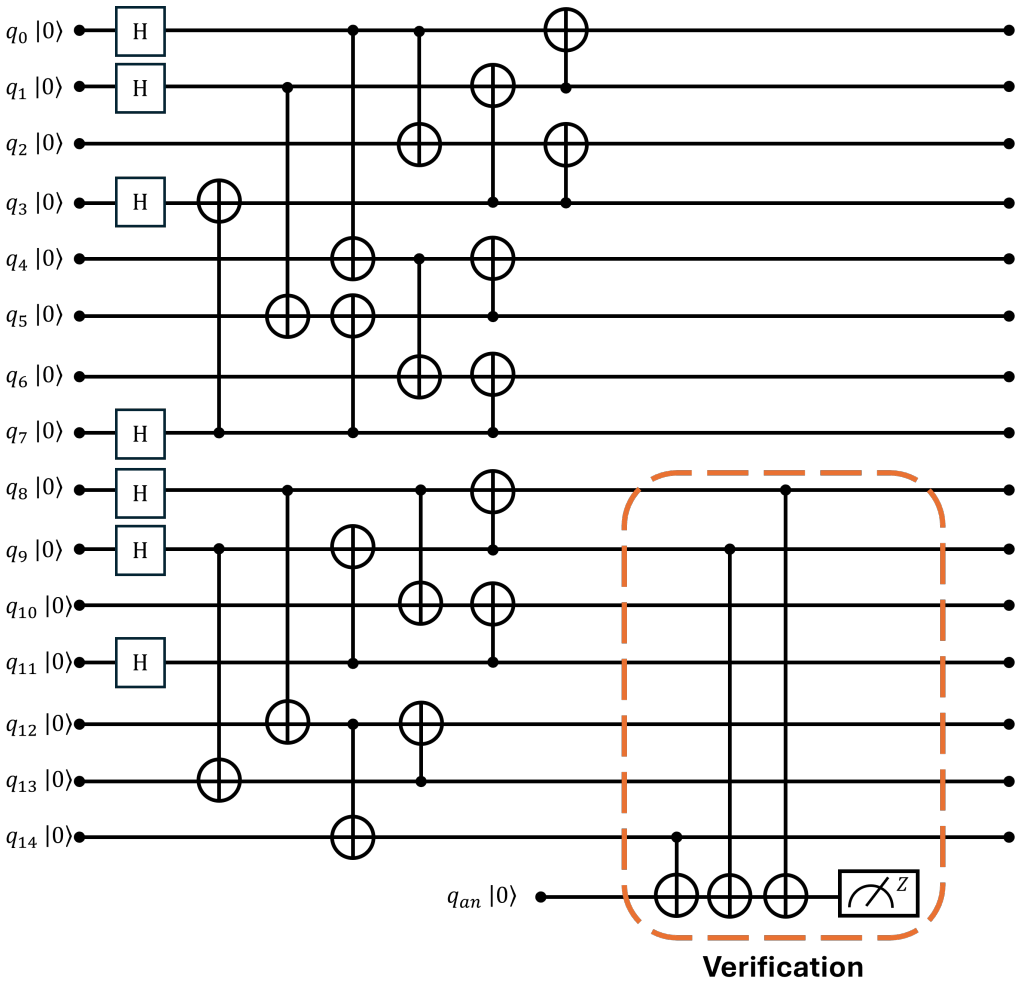

Figure 8: Circuit for initialization of $|0\rangle_L$ state on $\mathcal{Q}^{\mathrm{Sym}}$. The non-fault-tolerant encoding circuit is optimized by [29]. The verification procedure corresponding to measure out the logical $\mathbf{Z}_L = \mathbf{Z_9 Z_{10} Z_{15}}$ of symmetric code, and detect all uncorrectable high-weight Pauli-X errors. In total 22 CNOT gates are used, and for $|+\rangle_L$ state, one can simply add 15 transversal Hadamard gates in the end, since $\mathcal{Q}^{\mathrm{Sym}}$ has Hadamard gate transversality.